PARTICLE-SCALE MELT MODELING OF THE SELECTIVE LASER MELTING PROCESS

D. Moser*, M. Cullinan*, and J. Murthy†

*Department of Mechanical Engineering, University of Texas at Austin, Austin, TX

†Department of Mechanical Engineering, University of California Los Angeles, Los Angeles, CA

Abstract

In this work, a melting model is developed and implemented to simulate the melting of powder particles for Selective Laser Melting (SLS). A hybrid continuum-discrete methodology is used to model the melting process. A Discrete Element Model (DEM) is used to generate random packing structures of spherical particles. These structures are then placed on top of a background mesh in the OpenFOAM finite volume library. The radiation transport equation (RTE) is solved on the mesh to simulate the effect of laser heating. Heat sources generated by the RTE are introduced into the energy equation, which is also solved on the mesh. Once particle melting occurs, the resulting flow is solved for on the mesh. Computation of properties in the mesh cells is accomplished using volume averaging between the solid, liquid, and background gas phases. The resulting total melt pool depth and width is calculated and results compared against previously published experimental results and good agreement is obtained. Relations are then developed for the melt fraction of the powder as a function of the average temperature of the powder. These relations can be used as bulk properties in the enthalpy model for part-scale simulations.

Introduction

Free-form fabrication techniques reduce costs of creating prototypes or small batch parts by creating parts directly from CAD models. Selective Laser Melting (SLM) is a promising free-form fabrication process as it works with a wide variety of materials. SLM produces a solid object by selectively fusing successive layers of melt powder. A thin layer of powder is deposited on top of a piston. The surface of the powder is then scanned by a laser with a modulated power, fusing the powder to itself and the layer below where the cross-section is intended to be solid and leaving it lose where it is not. When the scan of the layer is complete, a new layer of powder is deposited on top and the process repeats. After the build is complete, the loose powder is removed, leaving the final part [1]. SLM processing parameters (laser power and speed, scan pattern, preheat temperature, etc.) have a strong influence on the quality of the produced part. However, it is often difficult to determine the optimal processing parameters for a given material and geometry. Thus, experimentation and testing is often required when using new materials or geometries to determine the parameters needed to produce an acceptable part.

Accurate computational models of the SLM process have the potential reduce the

experimentation and testing required in SLM. Continuum models, in which the powdered material is treated as a continuous medium as opposed to a collection of individual particles, are particularly promising in their ability to handle large domains without incurring prohibitive computational expense. Continuum models approximate SLM powder beds as a continuous medium as opposed to resolving individual powder particles and use effective material properties to capture the powdered nature of the medium.

Continuum models describe the heat transfer in the powder bed using the heat enthalpy formulation of the energy equation.

$$\frac{\partial H}{\partial t} = \nabla \cdot (k \nabla T) + f(x, y, z, t)$$

Equation 1

For closure, a relationship between the enthalpy of the powder and the temperature is required:

$$H = (1 - g(T)) \int_{T_{ref}}^{T} \rho c_s dT + g(T) \int_{T_{ref}}^{T} \rho c_l dT + g(T) \rho L$$

Equation 2

H is the enthalpy of the powder, k is the thermal conductivity, f is the laser heat source, c_s is the specific heat of the solid powder, c_l is the specific heat of the liquid metal, L is the latent heat of the powder, ρ is the density of the powder, and g(T) is the metal temperature-melt fraction function. While g(T) relations may be available in the literature for bulk materials, they are generally not for powdered materials. However, if the melting of a powder were simulated at the particle scale, such a relation could be calculated and applied in larger scale continuum models.

A number of groups have modeled the SLM process on the particle level. Korner et al. [2] developed a 2D lattice Boltzmann model of the melting of metal powder in SLM. Gurtler et al. [3] used a 3D volume of fluid method to model the melting process capable of simulating multiple laser passes. Khairallah and Anderson [4] developed a high resolution SLM model considering a number of phenomena. However, to our knowledge no groups have used the results from a particle-level SLM simulation to calculate a temperature-melt fraction relationship for use in a continuum model.

Modeling Approach
Powder Bed Generation

In order to calculate the temperature-melt fraction relationship, a powder bed is first generated using the discrete element method of the open source software MFiX. In the discrete element method (DEM), particles are modeled as a series of spherical control volumes, each with a position, radius, and velocity [5], [6]. Particle packings are created by inserting a chosen number of particles in a domain and allowing them to interact with other particles and respond to gravitational forces. Particles interact with each other using a spring-dashpot model in which contact forces are generated based on the degree of overlap a particle has with its neighbors

(described in detail by Garg et al. [5]). For the purposes of this work, the MFiX particle-particle interaction model is used simply as a means to generate a random packing of particles.

Once the particles settle, their positions and properties are used as an input for the melting model. The particle packing structure is placed on top of a finite volume mesh. For each mesh cell, the volume of overlap with each of the particles is calculated. The total volume of intersection with all the particles determines the volume faction, β, of solid material in that cell. Cells that are completely contained within a particle have solid volume fractions of 1.0. Cells not overlapping with particles at all have solid volume fractions of 0.0 and cells partially overlapped with particles have solid volume fractions between 0.0 and 1.0. In this way, the DEM representation of the particle bed is converted to a mesh representation that serves as an initial condition for the melting model.

Fluid Model

The melting model is a multiphase system consisting of three components: solid metal, liquid metal due to the melting of the particles from the laser, and a background gas. The motion of the system is modeled using a modified volume of fluid (VOF) method. The VOF method considers each mesh cell to contain a mixture of solid, liquid, and gas moving at a single mixture velocity. The mixture velocity is calculated using a form of the Navier-Stokes equations [7].

$$\frac{\partial \gamma \rho_m}{\partial t} + \nabla \cdot (\gamma \rho_m u_m) = S$$

Equation 3

$$\frac{\partial \gamma \rho_m u_m}{\partial t} + \nabla \cdot (\gamma \rho_m u_m u_m) = -\gamma \nabla P + \nabla \cdot (\gamma \tau) + \rho_m g + F_s - \epsilon \frac{(1-\gamma)^2}{\gamma^3} u_m$$

Equation 4

Here, γ is the volume fraction of the fluid, defined as 1.0-β, u_m is the mixture velocity, ρ_m is the mixture density, S is the source term due to melting, P is the pressure, τ is the fluid stress tensor, g is the gravitational acceleration and F_s is the surface tension force. The $\epsilon \frac{(1-\gamma)^2}{\gamma^3} u_m$ term is a momentum sink that drives the velocity of the mixture to zero in cells that are fully solid.

The fluid volume fraction, γ is calculated explicitly based on the initial distribution of solid material and the melting process discussed later. The volume fraction of liquid, α is tracked using the VOF advection equation.

$$\frac{\partial \gamma \alpha}{\partial t} + \nabla \cdot (\gamma u_m \alpha) = S$$

Equation 5

Equations 3, 4, and 5 are solved sequentially at each time step using the OpenFOAM finite volume solvers to evolve the mixture velocity and liquid volume fraction fields. The mixture properties required for the equations (ie. ρ_m) are calculated by volume averaging using the liquid

volume fraction field and the properties of the pure materials: $\rho_m = \alpha\rho_l + (1.0 - \alpha)\rho_g$, where ρ_l and ρ_g are the densities of the pure liquid and gas respectively.

Thermal and Melting Model

Heat transfer is accomplished using the enthalpy formulation of the energy equation.

$$\frac{\partial H_m}{\partial t} = \nabla \cdot (k_m \nabla T) + f(x, y, z, t)$$

Equation 6

This equation is the same as the one used in the large-scale continuum model of the process (Equation 1), except that now the mixture enthalpy is used. Similar to how mixture properties are determined for the fluid flow equations, H_m can be calculated using the solid, fluid, and liquid volume fraction fields: $H_m = (\beta + \gamma\alpha)H_{metal} + \gamma(1.0 - \alpha)H_{gas}$. The relation can now be closed using known relationships between the temperature and enthalpy of the metal and gas.

$$H_{metal} = (1 - g_{metal}(T)) \int_{T_{ref}}^{T} \rho_{metal} c_{metal,solid} dT + g_{metal}(T) \int_{T_{ref}}^{T} \rho_{metal} c_{metal,liquid} dT$$

$$+ g_{metal}(T) \rho_{metal} L_{metal}$$

Equation 7

$$H_{gas} = \int_{T_{ref}}^{T} \rho_{gas} c_{gas} dT$$

Equation 8

The energy equation is solved iteratively using the enthalpy method outlined by Swaminathan and Voller [8] in the OpenFOAM finite volume solver until the temperature and enthalpy fields are consistent. Finally, those cells containing metal whose temperatures cross the melting point of the metal are converted to solid or liquid, as appropriate, by explicitly updating the solid and fluid volume fraction fields (γ and β) and generating a source term for the VOF equation to update α, the liquid volume fraction field.

Radiation Model

Radiation is modeled using the radiation transport equation (RTE).

$$\nabla \cdot (I(\vec{x}, \vec{s})\vec{s}) + a_m I(\vec{x}, \vec{s}) = a_m \frac{\sigma T^4}{\pi}$$

Equation 9

$I(\vec{x}, \vec{s})$ is the radiation intensity field, a_m is the mixture absorptivity, and σ is the Stefan-Boltzman constant. The mixture absorptivity is calculated using the volume fraction fields: $a_m = (\beta + \gamma\alpha)a_{metal} + \gamma(1.0 - \alpha)a_{gas}$.

The RTE requires additional discretization within in the finite volume mesh, as the intensity field is a function of not only spatial location, but also direction. This discretization is done using the discrete ordinates method [9] in which the unit sphere is divided into a finite number of solid angles. The intensity field for each solid angle is solved for sequentially using the OpenFOAM finite volume solver and iterated until the fields are consistent. Once the intensity field is calculated, a source term is generated for the energy equation.

$$f(x, y, z, t) = a_m(G - 4\sigma T^4)$$

Equation 10

G is the sum of the intensity field over all of the solid angles.

The radiation due to the laser is handled as a boundary condition to the RTE at the topmost boundary of the domain. The intensity due to the laser is given by Equation 11.

$$I = \frac{2\epsilon P}{\pi\omega^2} e^{\frac{-2r^2}{\omega^2}}$$

Equation 11

ϵ is the emissivity of the metal, P is the laser power, ω is the characteristic radius, and r is the distance between the center of the laser and a given point on the boundary. The laser intensity is integrated over each cell on the boundary and applied as a fixed-value boundary condition in the RTE. This is shown in Figure 1.
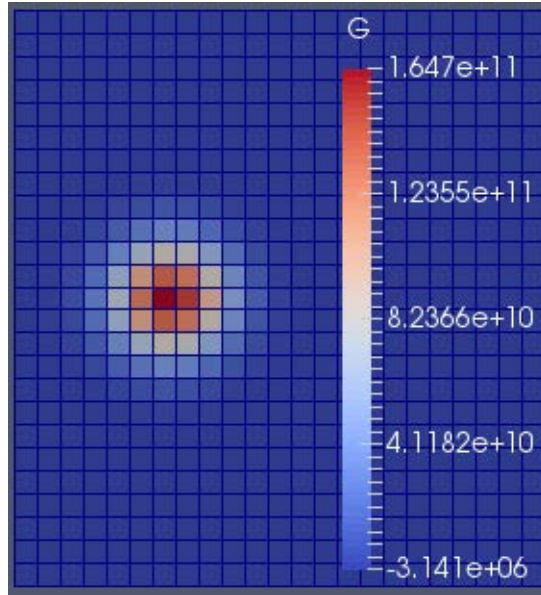

Figure 1: Laser Boundary Condition

As the laser beam is taken to be entering straight downwards into the domain, the boundary

condition is applied only to those solid angles for which $\vec{s} \cdot \vec{n}$ is approximately -1. The causes the laser intensity to propagate down into the domain as shown in Figure 2.
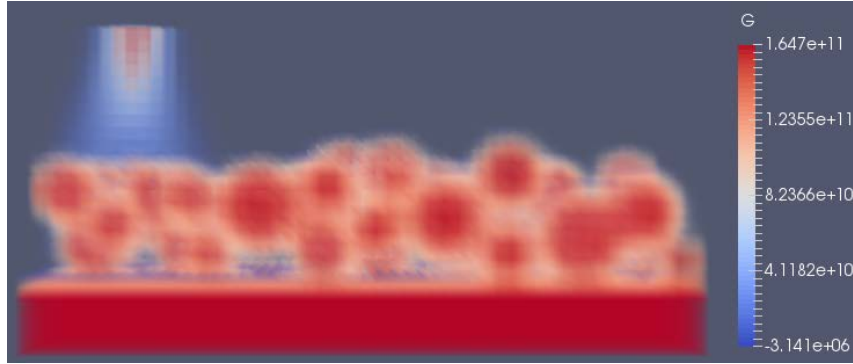

Figure 2: Laser Entering Domain

Results and Discussion
Model Validation

In order to assess the ability of the melting model to accurately predict SLM melt pool geometries, simulation results are compared to the experimental results of Gusarov et al. [10]. Gusarov et al. measured the melt pool depth and height of a 316 stainless steel plate due to laser irradiation. Material properties for 316 stainless steel are given by Khairallah and Anderson [4] and summarized in Table 1.

Property	Value
Density	7.43 g/cm^3
Viscosity	6.42 g/s m
Surface Tension	1.7 N/m
Thermal Conductivity	20.0 W/m K
Specific Heat	320.3 + 0.379T J/kg K
Emissivity	0.3

Table 1: 316 Stainless Steel Material Properties

Figure 3 shows the melt pool geometry measured by Gusarov et al. for a laser power of 25W and scanning speed of 15 cm/s. Figure 4 shows the melt pool geometry calculated using the melting model for the same laser power and scanning speed.
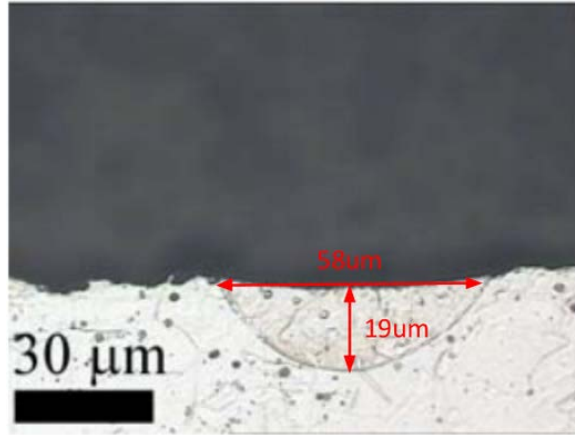
Figure 3: Melt Pool Geometry from Gusarov et al. (2009)

As can be seen, the calculated result of 60μm by 16μm shows good agreement with the experimental measurement of 58μm by 19μm. Uncertainties in the exact laser power, emissivity
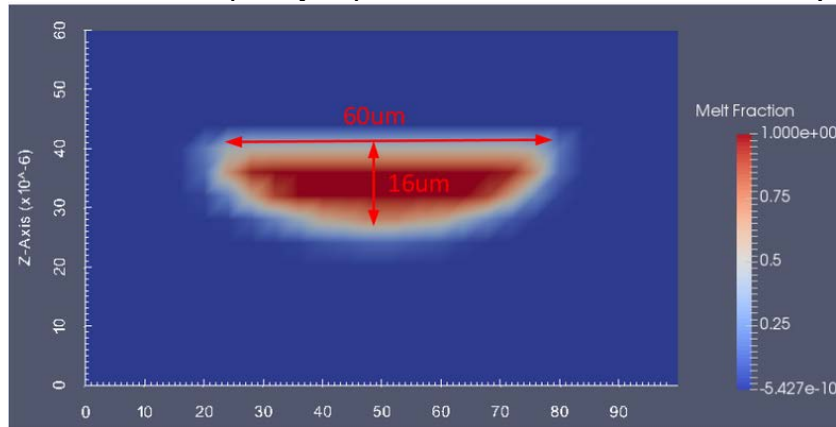

Figure 4: Melt Pool Geometry From Model Calculation

of the steel and diameter of the laser beam, as detailed in [10], likely account for the differences between the calculated and experimental results.

Calculation of Temperature-Melt Fraction Curve

In order to calculate the temperature-melt fraction curve, a simulation is run with a layer of 20μm diameter 316 stainless steel powder on top of a 316 stainless steel substrate scanned with a 200W laser at 2 m/s. Figure 5 shows the initial and final solid fraction configuration in the domain.
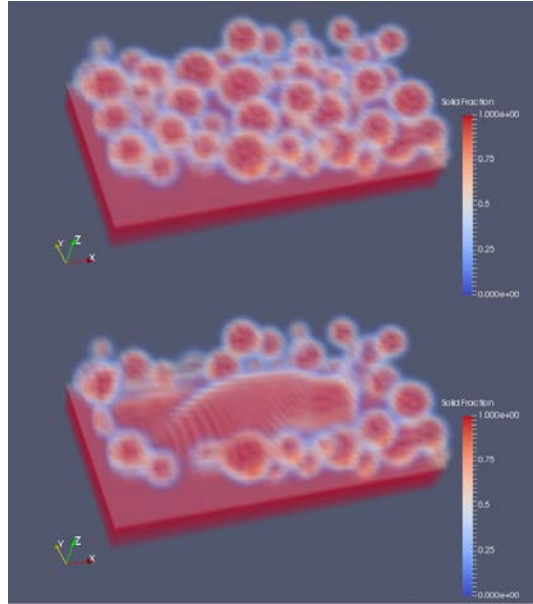
Figure 5: Initial and Final Solid Fraction Configuration

From the simulation results, a cubic domain element 1 layer thickness (40μm) on a side located in the center of the domain is considered. The temperatures of all the cells making up the element are averaged together to create an average temperature for the element at each time step. Similarly, the total fraction of liquid present in each cell ($\frac{\gamma\alpha}{\beta+\gamma\alpha}$) is averaged over each cell in the element to create an average melt fraction for the element at each time step. The resulting curve is shown in Figure 6 along with the temperature-melt fraction curve of pure solid stainless steel.
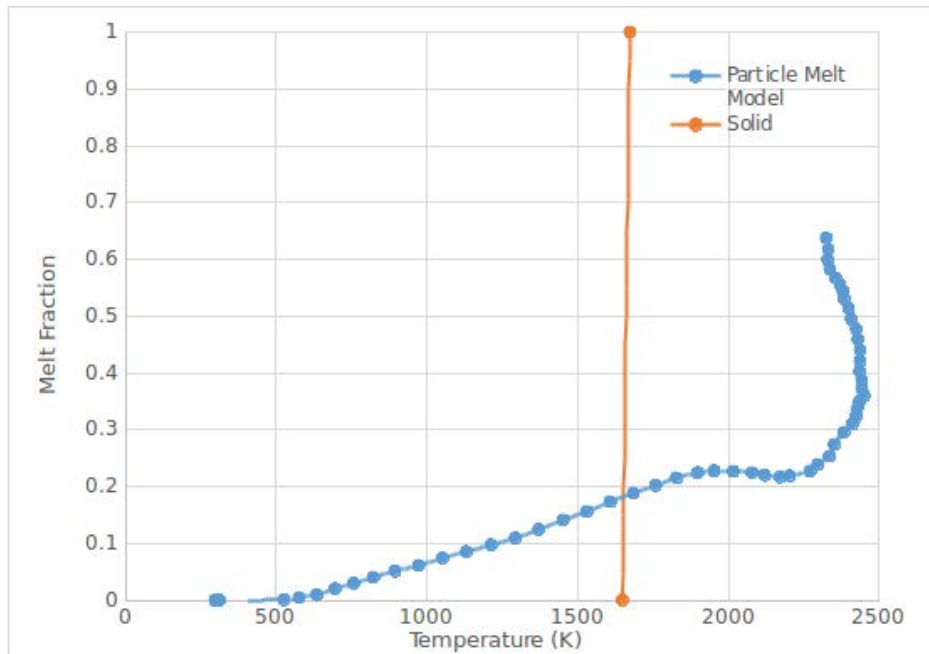

Figure 6: Average Melt Fraction vs Average Temperature

As can be seen, the powdered stainless steel exhibits very different melting behavior than the bulk solid. Since the powder heats up unevenly due to the laser, small amounts of melt form at very low average temperatures, as only the very top of the material has reached the melt temperature while the material below is significantly cooler. The melting process also takes much longer to occur as the melt forming at the top shields the remaining material from the laser heat. Finally, once the melted material at the top of the element begins to move, it mixes with the cooler material below, melting it and also allowing additional laser radiation to penetrate, leading to more rapid melting towards the end of the process. Thus, it can be seen that approximating the temperature-melt fraction curve of a powder with a simple linear relationship would introduce significant errors in the melting behavior. Using temperature-melt fraction curves calculated from detailed, powder-level melting models as in Figure 6 should allow a more accurate representation of melt behavior in large-scale SLM continuum models.

Conclusions

A particle scale melting model of an SLM powder bed is developed and implemented using MFiX-DEM and OpenFOAM. MFiX-DEM is used to generate particle packing structures which are then converted to a mesh representation and imported into the OpenFOAM finite volume framework in which the model governing equations for fluid flow, heat transfer, and radiation are solved. Results from the model are compared against experimental measurements for laser irradiation on a stainless steel plate and good agreement is obtained. The model is used to predict the melt behavior of stainless steel powder undergoing laser melting. From this, it is shown that the average temperature-melt fraction relationship predicted by model is significantly different than the linear extrapolation typically used for bulk materials. This more complex relationship can be used to inform a more accurate temperature-melt fraction function for use in large scale SLM continuum models. Future work includes the quantification of uncertainties in the model due to uncertainties in the inputs, an examination of the dependency of the temperature-melt fraction function on the laser power and speed and a quantification of the error introduced when using a calculated temperature-melt fraction curve in a large scale continuum model.

Bibliography

[1]   J. C. Nelson, S. Xue, J. W. Barlow, J. J. Beaman, H. L. Marcus, and D. L. Bourell, "Model of the selective laser sintering of bisphenol-A polycarbonate," *Ind. Eng. Chem. Res.*, vol. 32, no. 10, pp. 2305–2317, Oct. 1993.

[2]   C. Körner, E. Attar, and P. Heinl, "Mesoscopic simulation of selective beam melting processes," *J. Mater. Process. Technol.*, vol. 211, no. 6, pp. 978–987, 2011.

[3]   F.-J. Gürtler, M. Karg, K.-H. Leitz, and M. Schmidt, "Simulation of Laser Beam Melting of Steel Powders using the Three-Dimensional Volume of Fluid Method," *Phys. Procedia*, vol. 41, pp. 881–886, 2013.

[4]   S. A. Khairallah and A. Anderson, "Mesoscopic simulation model of selective laser melting of stainless steel powder," *J. Mater. Process. Technol.*, vol. 214, no. 11, pp. 2627–2636, 2014.

[5]   R. Garg, J. Galvin, T. Li, and S. Pannala, "Documentation of open-source MFIX–DEM software for gas-solids flows," 2012. [Online]. Available: https://mfix.netl.doe.gov/documentation/dem_doc_2012-1.pdf. [Accessed: 08-Oct-2014].

[6]   J. M. H. Musser, "Modeling of Heat Transfer and Reactive Chemistry for Particles in Gas-Solid Flow Utilizing Continuum-Discrete Methodology (CDM)," West Virginia University, 2011.

[7]   N. Iqbal and C. Rauh, "Coupling of discrete element model (DEM) with computational fluid mechanics (CFD): A validation study," *Appl. Math. Comput.*, vol. 277, pp. 154–163, 2016.

[8]   C. R. Swaminathan and V. R. Voller, "A general enthalpy method for modeling solidification processes," *Metall. Trans. B*, vol. 23, no. 5, pp. 651–664, 1992.

[9]   J. Y. Murthy and S. R. Mathur, "Finite Volume Method for Radiative Heat Transfer Using Unstructured Meshes," *J. Thermophys. Heat Transf.*, vol. 12, no. 3, pp. 313–321, Jul. 1998.

[10]   A. V Gusarov, I. Yadroitsev, P. Bertrand, and I. Smurov, "Model of Radiation and Heat Transfer in Laser-Powder Interaction Zone at Selective Laser Melting," *J. Heat Transfer*, vol. 131, no. 7, p. 72101, May 2009.